The appearance and duration of the Jehol Biota: Constraint from SIMS U-Pb zircon dating for the Huajiying Formation in northern China

Saihong Yang[a,b], Huaiyu He[a,b,c,1], Fan Jin[d], Fucheng Zhang[e], Yuanbao Wu[f], Zhiqiang Yu[a,b,c], Qiuli Li[a,b,c], Min Wang[d,g], Jingmai K. O'Connor[d,g], Chenglong Deng[a,b,c], Rixiang Zhu[a,b,c], and Zhonghe Zhou[d,g,1]

[a]State Key Laboratory of Lithospheric Evolution, Institute of Geology and Geophysics, Chinese Academy of Sciences, 100029 Beijing, China; [b]Institutions of Earth Science, Chinese Academy of Sciences, 100029 Beijing, China; [c]College of Earth and Planetary Sciences, University of Chinese Academy of Sciences, 100049 Beijing, China; [d]Key Laboratory of Vertebrate Evolution and Human Origins of Chinese Academy of Sciences, Institute of Vertebrate Paleontology and Paleoanthropology, Chinese Academy of Sciences, 100044 Beijing, China; [e]Institute of Geology and Paleontology, Linyi University, 276000 Linyi, Shandong, China; [f]State Key Laboratory of Geological Processes and Mineral Resources, Faculty of Earth Sciences, China University of Geosciences, 430074 Wuhan, China; and [g]Center for Excellence in Life and Paleoenvironment, Chinese Academy of Sciences, 100044 Beijing, China

Contributed by Zhonghe Zhou, March 29, 2020 (sent for review October 23, 2019; reviewed by Xiumian Hu and Alexander Nemchin)

The Lower Cretaceous Huajiying Formation of the Sichakou Basin in northern Hebei Province, northern China contains key vertebrate taxa of the early Jehol Biota, e.g., *Protopteryx fengningensis*, *Archaeornithura meemannae*, *Peipiaosteus fengningensis*, and *Eoconfuciusornis zhengi*. This formation arguably documents the second-oldest bird-bearing horizon, producing the oldest fossil records of the two major Mesozoic avian groups Enantiornithes and Ornithuromorpha. Hence, precisely determining the depositional ages of the Huajiying Formation would advance our understanding of the evolutionary history of the Jehol Biota. Here we present secondary ion mass spectrometry (SIMS) U-Pb zircon analysis results of eight interbedded tuff/tuffaceous sandstone samples from the Huajiying Formation. Our findings, combined with previous radiometric dates, suggest that the oldest enantiornithine and ornithuromorph birds in the Jehol Biota are ∼129–131 Ma, and that the Jehol Biota most likely first appeared at ∼135 Ma. This expands the biota's temporal distribution from late Valanginian to middle Aptian with a time span of about 15 My.

Jehol Biota | Cretaceous | U-Pb geochronology

The Jehol Biota in eastern Asia contains a plethora of evidence regarding terrestrial ecosystems during the Early Cretaceous. It comprises representatives of almost all of the major clades of Early Cretaceous terrestrial and freshwater vertebrates, a wide variety of invertebrates, and a diverse flora (1–6). It has produced a wealth of spectacular fossils, including feathered dinosaurs, early birds, mammals, pterosaurs, and amphibians, as well as an abundance of insects and early flowering plants, thus providing a unique window for probing into the evolutionary process of this Early Cretaceous terrestrial ecosystem (1, 5).

A consensus has not yet been reached regarding a definition for the Jehol Biota, thus hindering our study of its spatiotemporal distribution, diversity, and pattern of radiation (4, 5, 7). Taking into account ecological and taphonomic aspects, Pan et al. (7) proposed a definition for the Jehol Biota, representing "the organisms that lived in Early Cretaceous volcanic-influenced environments of northeastern China, and were buried in lacustrine and, rarely, fluvial sediments, where most turned into exceptionally preserved fossils," which is followed in this study.

Based on this definition, the Jehol Biota consists of fossils from the Yixian and Jiufotang formations in western Liaoning and southern Inner Mongolia, and the Huajiying Formation in northern Hebei (5) (Fig. 1). In those areas, the exceptionally fossiliferous Early Cretaceous sequences of terrestrial sediments intercalated with numerous layers of tuffs and tuffaceous clastic rocks hold great promise for radiometric dating. Considerable progress has been made during the past two decades toward radiometrically dating the Yixian and Jiufotang formations, and hence chronologies of the middle and late stages of the Jehol Biota have been well established (8–13).

Research efforts have been made to radiometrically constrain the age of the early stage of the Jehol Biota preserved in the Huajiying Formation (formerly the Dabeigou Formation) of northern Hebei (14). Nevertheless, high-precision dates remain sparse and a chronological consensus of the Early Jehol Biota has not yet been reached. The lack of precise age constraints on the deposition of the Huajiying Formation and associated Early Jehol Biota hinders our understanding of the timing of key ecological differentiation and radiation, and their relationship with ecological processes of the Early Cretaceous terrestrial ecosystem. Therefore, systematic dating of the tuff and tuffaceous layers in the Huajiying Formation, which has produced fewer but important fossils belonging to the earliest stage of the Jehol Biota, is required in order to precisely constrain the age of the Huajiying Formation and the taxa it contains.

The strata bearing the earliest Jehol Biota are found in the Sichakou and Senjitu basins in northern Hebei, and consist of

Significance

The Jehol Biota is well known for producing exceptionally preserved specimens of feathered dinosaurs, early birds, mammals, as well as insects and early flowering plants, thus providing key evidence for understanding the early evolution of birds and for reconstructing the Early Cretaceous terrestrial ecosystem. Here, we present eight SIMS U-Pb zircon ages from the Huajiying Formation, the lowest Jehol fossil-bearing deposits in northern China, which have placed stringent age controls on the early phase of the Jehol Biota, and have extended the temporal range of the Jehol Biota to over 15 My. Our findings will shed light on the evolutionary radiation of the Jehol Biota as well as the origins of major vertebrate groups in the Early Cretaceous.

Author contributions: H.H., R.Z., and Z.Z. designed research; S.Y., H.H., C.D., and Z.Z. performed research; S.Y., H.H., Y.W., Z.Y., and Q.L. analyzed data; S.Y., H.H., F.J., and F.Z. collected samples; and S.Y., H.H., M.W., J.K.O., and C.D. wrote the paper.

Reviewers: X.H., Nanjing University; and A.N., Curtin University.

The authors declare no competing interest.

Data deposition: The SIMS U-Pb age data in this paper are available in EarthRef Digital Archive, https://earthref.org/ERDA/2421/.

[1]To whom correspondence may be addressed. Email: huaiyuhe@mail.iggcas.ac.cn or zhouzhonghe@ivpp.ac.cn.

This article contains supporting information online at https://www.pnas.org/lookup/suppl/doi:10.1073/pnas.1918272117/-/DCSupplemental.

First published June 8, 2020.

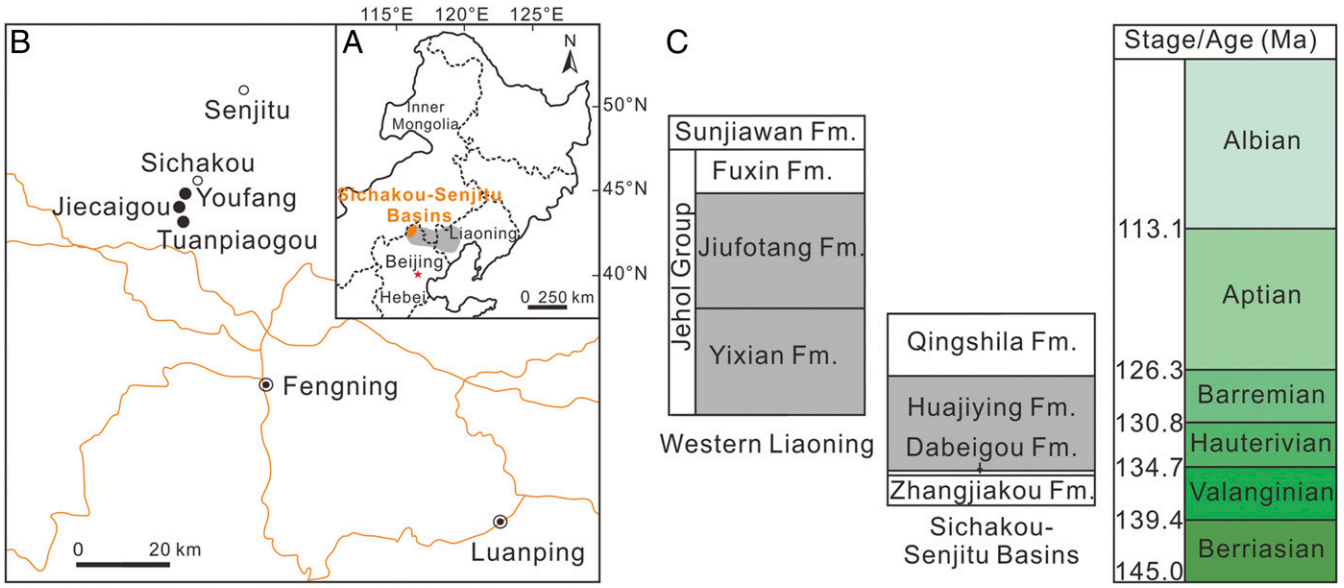

Fig. 1. Spatial and temporal distribution of the Jehol Biota reprinted from ref. 7, copyright (2013), with permission from Elsevier and from ref. 5, which is licensed under CC BY 4.0. The international chronostratigraphic chart of Lower Cretaceous was after Ogg et al. (32). (*A*) The area yielding the Jehol Biota. (*B*) Locations of the studied sections. (*C*) Chronostratigraphic and lithostratigraphic position of the Jehol Biota in western Liaoning and northern Hebei.

sedimentary sequences of fluvio-lacustrine and lacustrine deposits with abundant pyroclastics (15) (Figs. 1 and 2). Notably, the fossil-bearing sedimentary layers in the Sichakou Basin are biochronologically older than those in the Senjitu Basin (15). In this paper, we report secondary ion mass spectrometry (SIMS) U-Pb zircon ages from eight tuffs/tuffaceous sandstone layers in the Sichakou Basin (Figs. 2–5), providing precise chronological calibration and constraint on the lower Huajiying Formation, which contains key taxa of the Early Jehol Biota, e.g., *Protopteryx fengningensis* (the basalmost enantiornithine bird) (16), *Archaeornithura meemannae* (the oldest ornithuromorph bird) (17), *Eopengornis martini* (a basal enantiornithine bird) (18), *Eoconfuciusornis zhengi* (the basalmost confuciusornithid bird) (19), *Cruralispennia multidonta* (a derived enantiornithine bird with a modern birdlike tail bone) (20), and *Peipiaosteus fengningensis* and *Yanosteus longidorsalis* (basal acipenseriform fish) (15). Combining our findings obtained from the Huajiying Formation in northern Hebei, along with a series of published radiometric dates obtained from the Yixian and Jiufotang formations in western Liaoning (8–13), we are now able to precisely determine the appearance and duration of the Jehol Biota.

Geology of the Sichakou Basin

The Sichakou Basin (Fig. 1) in Fengning County, northern Hebei Province is located in the northern part of the Yanshan Fold and Thrust Belt, which is the eastern segment of a major east–west-trending Jurassic–Cretaceous orogenic system and comprises the northern part of the North China Craton (21). During the Late Mesozoic, multiple phases of folding, contractional, extensional, and strike-slip faulting resulted in widespread occurrence of terrestrial sedimentation, magmatism, and deformation in the Yanshan Fold and Thrust Belt (21). The Sichakou Basin is one of the volcanic and sedimentary basins formed during the Late Mesozoic in this region.

In the Sichakou Basin, the Late Mesozoic terrestrial strata, comprising volcanic, volcanoclastic, and sedimentary rocks (Fig. 2), consist of three lithologic formations, from bottom to top: the Zhangjiakou, Dabeigou, and Huajiying formations (Figs. 1*C* and 3) (15). The Zhangjiakou Formation mainly consists of volcanic rocks, e.g., rhyolitic ignimbrite, rhyolite, and quartz trachyte. The Dabeigou Formation, which was named in the Luanping Basin (22), mainly consists of sandy conglomerates and conglomeratic sands sometimes overlain by lacustrine siltstones. The Huajiying Formation mainly comprises fluvio-lacustrine and lacustrine siltstones interbedded with numerous layers of tuffs and tuffaceous clastic rocks. Key specimens of the Early Jehol Biota were preserved in great fidelity in the lacustrine shales of the Huajiying Formation (Fig. 3). The Qingshila Formation,

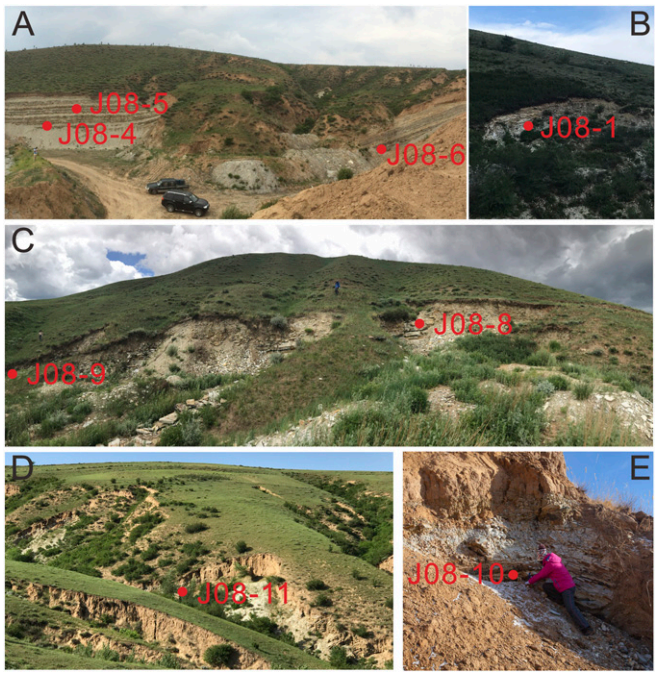

Fig. 2. Photos showing outcrops of the Youfang (*A* and *B*), Tuanpiaogou (*C*), and Jiecaigou (*D* and *E*) sections as well as sampling positions of the dated samples.

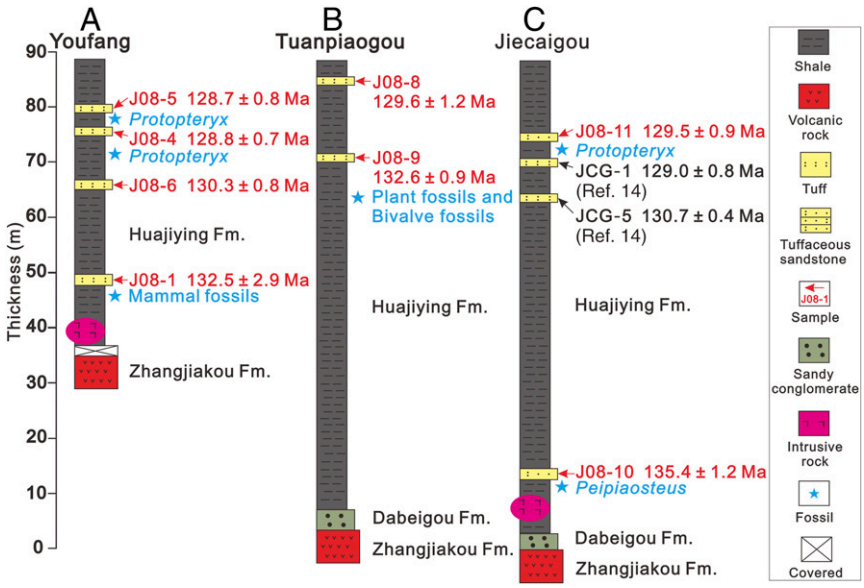

Fig. 3. Stratigraphy and geochronology of the Youfang (*A*), Tuanpiaogou (*B*), and Jiecaigou (*C*) sections. The arrows indicate the positions of the radiometrically dated horizons. The stars show the positions of fossils.

which is distributed in the Senjitu Basin, is absent in the Sichakou Basin (Fig. 1).

Samples

Eight samples were collected from the intercalated tuff and tuffaceous layers in the fluvio-lacustrine and lacustrine sedimentary sequences of the Huajiying Formation in the Sichakou Basin (Figs. 2 and 3). All of the samples were collected from excavated areas of the Youfang, Tuanpiaogou, and Jiecaigou sections, where outcrops are well exposed (Fig. 2). This permits clear and direct stratigraphic arrangement between the fossil-bearing shales and the intercalated tuff and tuffaceous layers, thus allowing us to precisely determine the ages of the strata and associated fossils. These sampling localities are less than 4 km apart. Active volcanic activities, folding, and faulting leave lithostratigraphic correlations between the three sections unclear. However, fossils in this region are abundant, facilitating biostratigraphic correlation.

Four samples are from the Youfang section (41°39′N, 116°21′E) (Figs. 2 *A* and *B* and 3*A*). Sample J08-1 was collected from a yellowish-white tuff layer (about 15 cm thick). Sample J08-4 was collected from a grayish-yellow tuff layer (about 5 cm thick), which lies between the *Protopteryx*-bearing shale layers (15, 16). Sample J08-5 was collected from a tuff layer interbedded in lacustrine shales (about 10 cm thick). Sample J08-6 was collected from a yellow tuff layer interbedded in lacustrine shales (about 3 cm thick), which underlies the bird fossil-bearing layer below sample J08-4.

Two samples are from the upper part of the Tuanpiaogou section (41°37′N, 116°21′E) (Figs. 2*C* and 3*B*). Sample J08-8 was collected from a white tuff layer and sample J08-9 was from a yellow tuff layer. Both samples were interbedded in lacustrine shales. The lacustrine shale layer ∼7.5 m below sample J08-9 yields abundant plant and bivalve fossils.

Two samples are from the Jiecaigou section (41°38′N, 116°21′E) (Figs. 2 *D* and *E* and 3*C*). Sample J08-10 was collected from a white tuffaceous sandstone layer in the lower part of the section, which is about 3 m above the lacustrine shale layer containing acipenseriform fossils (15). Sample J08-11 was collected from a grayish-yellow tuffaceous sandstone layer in the upper part of the section, which is about 1 m above the lacustrine shale layer containing *Protopteryx* (15, 16).

All of the collected samples are slightly altered and without fresh feldspars, and not suitable for Ar-Ar dating. Thus, we employed SIMS U-Pb dating on zircons to retrieve age estimates for the samples.

SIMS U-Pb Zircon Geochronology

Zircon Morphology. Zircon grains from the eight samples are mostly euhedral to subhedral, transparent and colorless, and have length to width ratios between 1:1 and 3:1. Most of the crystals have oscillatory zoning under cathodoluminescence (CL) images (Fig. 4), indicative of magmatic origin (23), while a minority has inherited cores, which are easily recognizable from the CL images (24) and not analyzed.

Sample J08-1. Eleven analyses were conducted on 11 zircons from sample J08-1. Eight of the 11 analyses have high Th/U ratios of 0.63–1.87 and indistinguishable $^{206}Pb/^{238}U$ isotopic ratios within analytical uncertainties. They yield a weighted mean $^{206}Pb/^{238}U$ age of 132.5 ± 2.9 Ma (mean standard weighted deviation [MSWD] = 3.0) (Fig. 5*A*), which is interpreted as the crystallization age of sample J08-1. Analysis spot 4 is performed on an inherited core, yielding a $^{207}Pb/^{206}Pb$ age of 2498.7 ± 12.3 Ma (*SI Appendix*, Table S1). Grains 2 and 6 are idiomorphic in shape and show oscillatory zoning under CL images. They have apparently old $^{206}Pb/^{238}U$ ages of 261.7 ± 3.8 Ma and 317.3 ± 4.8 Ma, respectively (*SI Appendix*, Table S1). These are all interpreted as xenocrysts.

Sample J08-4. Twenty-eight analyses were conducted on 27 zircon grains from sample J08-4. All of the 28 analyses have Th/U ratios of 0.49–0.99 and yield concordant to nearly concordant U-Pb ages. Except for analysis spot 7 that gives a slightly younger $^{206}Pb/^{238}U$ age of 123.6 ± 2.0 Ma (*SI Appendix*, Table S1), probably due to Pb loss (25), the remaining 27 analyses show indistinguishable $^{206}Pb/^{238}U$ isotopic ratios within analytical uncertainties, yielding a weighted mean of 128.8 ± 0.7 Ma (MSWD = 0.2) (Fig. 5*B*), which is interpreted as the crystallization age of sample J08-4.

Sample J08-5. Thirty analyses were conducted on 30 zircon crystals from sample J08-5 (Fig. 5*D*). The zircons of spots 8, 18, and 22 are idiomorphic grains showing oscillatory zoning under CL

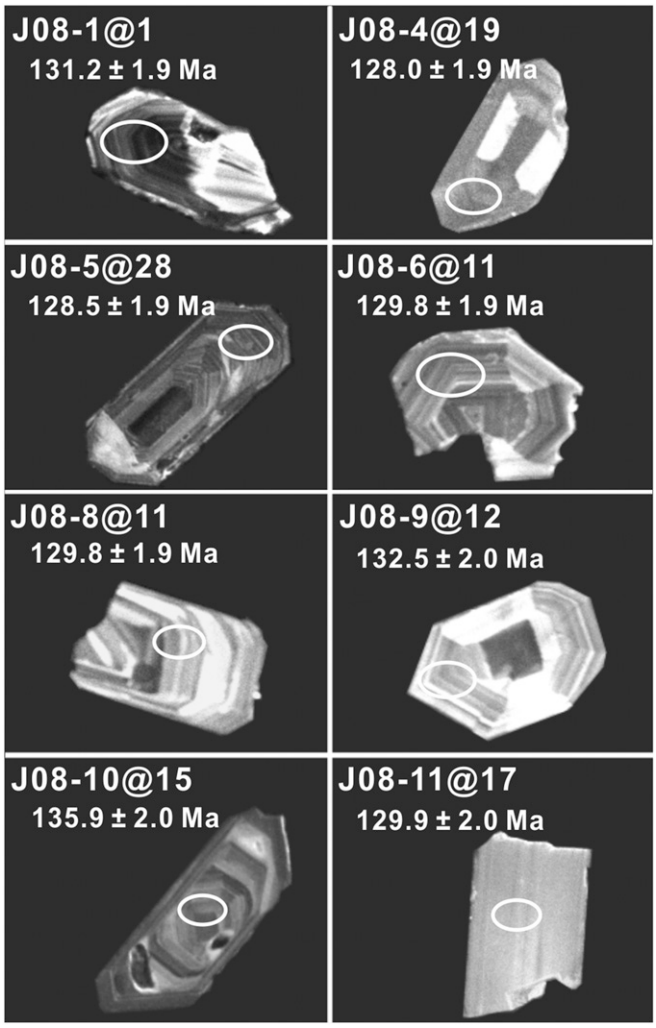

Fig. 4. CL images of representative zircons for in situ SIMS U-Pb dating. SIMS spots are 30 μm in length for scale. See Figs. 2 and 3 for sections and stratigraphic positions of the samples.

images, which give $^{206}Pb/^{238}U$ ages of 144.6 ± 2.6 Ma, 157.3 ± 2.4 Ma, and 196.4 ± 2.9 Ma, respectively (*SI Appendix*, Table S1). They are interpreted as xenocrysts. One analysis spot yields a slightly younger $^{206}Pb/^{238}U$ age of 119.6 ± 2.1 Ma, likely due to partial loss of radiogenic Pb (25). The remaining 26 analyses give concordant U-Pb ages and yield a weighted mean $^{206}Pb/^{238}U$ age of 128.7 ± 0.8 Ma (MSWD = 0.2) (Fig. 5*C*), which is interpreted as the crystallization age of sample J08-5.

Sample J08-6. Twenty-five analyses were conducted on 25 zircon grains from sample J08-6. All of the 25 analyses have indistinguishable $^{206}Pb/^{238}U$ isotopic ratios within analytical uncertainties. Among them, analysis spot 25 has a relatively high f_{206} ratio ($f_{206}\%$ = 3.01), implying a high common Pb content (25). The remaining 24 analyses give concordant U-Pb ages and yield a weighted mean $^{206}Pb/^{238}U$ age of 130.3 ± 0.8 Ma (MSWD = 0.9) (Fig. 5*E*), which is interpreted as the crystallization age of sample J08-6.

Sample J08-8. Twenty-two analyses were conducted on 22 zircons from sample J08-8 (Fig. 5*F*). Twenty-one of them are concordant with apparent $^{206}Pb/^{238}U$ ages varying from 127.9 ± 1.9 Ma to 145.5 ± 2.2 Ma, yielding a weighted mean of 132.9 ± 2.2 Ma (MSWD = 5.6). The high MSWD value means that the 21 analyses include different age groups. In the probability density diagram, 11 analyses form a main peak (Fig. 5*G*). These 11 analyses give a weighted mean $^{206}Pb/^{238}U$ age of 129.6 ± 1.2 Ma (MSWD = 0.5) (Fig. 5*H*), which is interpreted as the crystallization age of sample J08-8. Analysis spot 8 is performed on an idiomorphic zircon with oscillatory zoning, and gives a relatively old U-Pb age of 240.5 ± 3.6 Ma (*SI Appendix*, Table S1). It is thought to be a xenocryst.

Sample J08-9. Twenty analyses were conducted on 20 zircons from sample J08-9 (Fig. 5*I*). Analysis spot 7 is done on an idiomorphic zircon showing oscillatory zoning under CL images, and gives a $^{206}Pb/^{238}U$ age of 245.9 ± 3.7 Ma (*SI Appendix*, Table S1). It is thought to be a xenocryst. Grain 20 shows strong luminescence and has low U (58 ppm) and Th (56 ppm) contents, with a relatively young $^{206}Pb/^{238}U$ age of 128.9 ± 2.2 Ma (*SI Appendix*, Table S1), indicative of partial loss of radiogenic Pb (25). The other 18 analyses have indistinguishable U-Pb ages within analytical errors, yielding a weighted mean $^{206}Pb/^{238}U$ age of 132.6 ± 0.9 Ma (MSWD = 0.6) (Fig. 5*J*), which is interpreted as the crystallization age of sample J08-9.

Sample J08-10. Twenty-one analyses were conducted on 21 zircons from sample J08-10. Analysis spot 4 is performed on an inherited core, yielding a $^{207}Pb/^{206}Pb$ age of 1,950.9 ± 4.8 Ma. The remaining 20 analyses display two age groups (Fig. 5 *K* and *L*). Among them, 12 analyses yield indistinguishable U-Pb isotopic compositions within analytical errors, giving a weighted mean $^{206}Pb/^{238}U$ age of 135.4 ± 1.2 Ma and Th/U ratios of 0.39–1.03. Generally, the youngest age group obtained from magmatic zircons in tuff samples should represent the eruptive age of the tuff. The age of 135.4 ± 1.2 Ma (MSWD = 0.5) is thus interpreted as the crystallization age of sample J08-10, constraining the depositional age of the sampling horizon. The remaining eight analyses give a weighted mean $^{206}Pb/^{238}U$ age of 142.6 ± 1.5 Ma (MSWD = 0.6). This age may have recorded an earlier magmatic activity before the eruption of the tuff.

Sample J08-11. Twenty analyses were conducted on 20 zircons from sample J08-11 (Fig. 5*M*). Among them, grain 1 shows oscillatory zoning under CL images, and gives a relatively old $^{206}Pb/^{238}U$ age of 148.2 ± 2.2 Ma (*SI Appendix*, Table S1). It is thought to be a xenocryst. The other concordant 19 analyses have indistinguishable U-Pb isotopic compositions within analytical errors, giving a weighted mean $^{206}Pb/^{238}U$ age of 129.5 ± 0.9 Ma (MSWD = 0.4) (Fig. 5*N*), which is interpreted as the crystallization age of sample J08-11.

Discussion

Geochronology. All of the analyses were conducted on portions of zircon with oscillatory zoning, which is interpreted as reflecting growth in magma. The residence time of magma in the magma chamber is usually less than 200 kyr (26). In addition, the accuracy of the SIMS U-Pb dating method used in this study usually amounts to ~1% (27, 28). Thus, the magnitude of the residence time bias appears to be low relative to the Early Cretaceous Age of the dated samples, and the crystallization ages of the zircons approximate to their eruption ages. The consistency between the obtained ages from the tuff or tuffaceous sandstone samples and the stratigraphic sequences also indicate that the crystallization ages of zircons represent the depositional ages of the sampling horizons (Fig. 3). Thus, we considered that our SIMS U-Pb dates place stringent age constraints on the Huajiying Formation of the lower Jehol Group which bears the Early Jehol Biota.

The concordant zircon U-Pb ages of 128.7 ± 0.8 Ma (sample J08-5), 128.8 ± 0.7 Ma (sample J08-4), and 130.3 ± 0.8 Ma (sample J08-6) for the Youfang section (Fig. 3*A*), of 129.6 ± 1.2 Ma

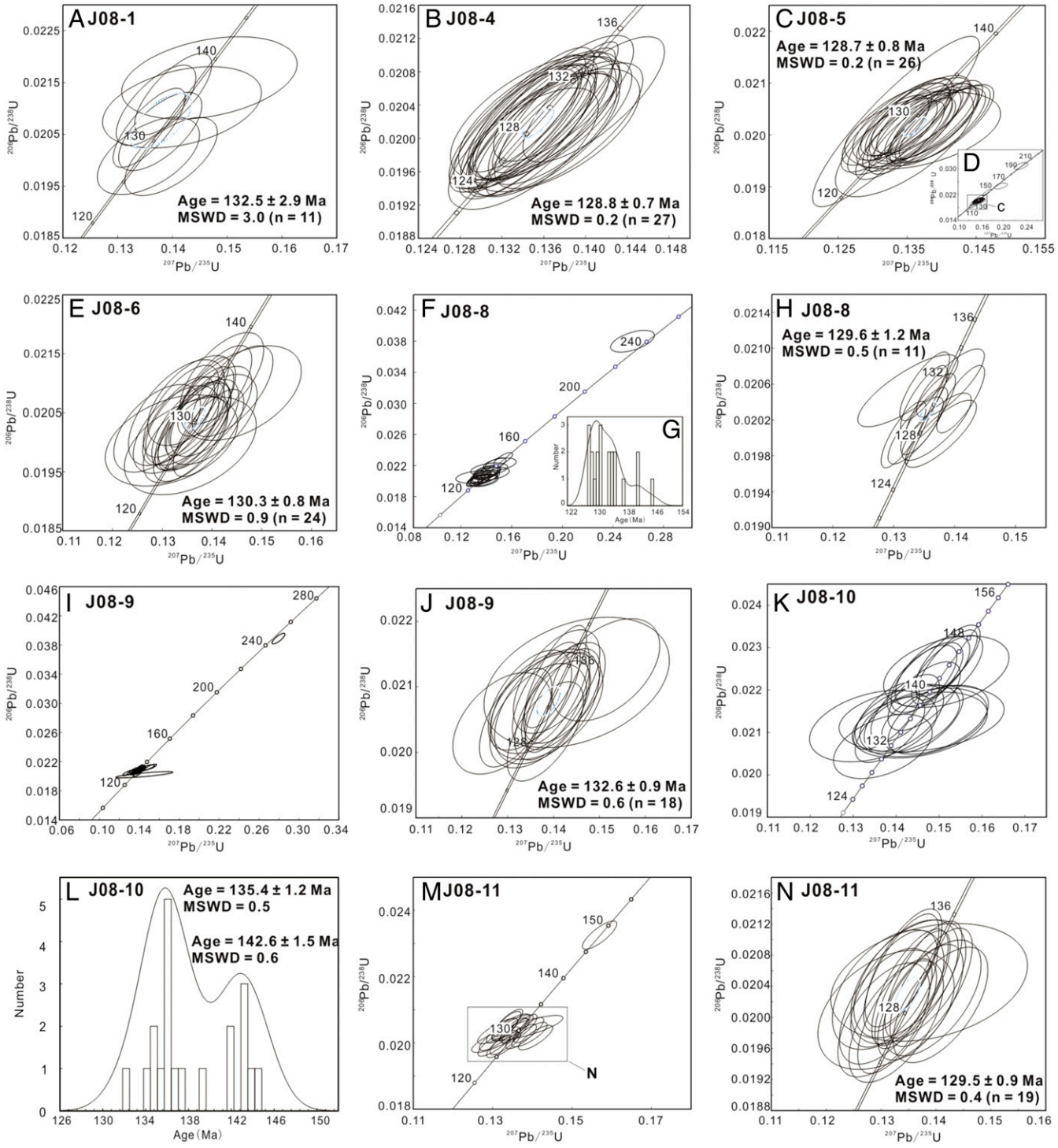

Fig. 5. SIMS U-Pb concordia age plots for zircons. (*A*–*E*) Samples of the Youfang section. (*F*–*J*) Samples of the Tuanpiaogou section. (*K*–*N*) Samples of the Jiecaigou section. See Figs. 2 and 3 for sections and stratigraphic positions of the samples.

(sample J08-8) for the Tuanpiaogou section (Fig. 3*B*), and of 129.5 ± 0.9 Ma (sample J08-11) for the Jiecaigou section (Fig. 3*C*) from five tuff/tuffaceous sandstone samples suggest that the fossil-bird-bearing layers were deposited at ∼129–130 Ma. The concordant zircon U-Pb ages of 132.5 ± 2.9 Ma (sample J08-1) for the Youfang section (Fig. 3*A*), 132.6 ± 0.9 Ma (sample J08-9) for the Tuanpiaogou section (Fig. 3*B*), and 135.4 ± 1.2 Ma (sample J08-10) for the Jiecaigou section (Fig. 3*C*) from three tuff or tuffaceous sandstone samples suggest that the sedimentary layers bearing mammalian fossils and acipenseriform fossils were deposited at ∼132–135 Ma. The similar age pattern of the Youfang, Tuanpiaogou, and Jiecaigou sections allows for a correlation of the fossil-bearing beds.

Notably, in the Jiecaigou section our SIMS U-Pb zircon dates are strongly consistent with previously obtained $^{40}Ar/^{39}Ar$ dates within errors (Fig. 3*C*). The SIMS U-Pb zircon age of 129.5 ± 0.9 Ma for sample J08-11, which lies ∼1 m above the lacustrine

shale layer containing *Protopteryx* (15, 16), is consistent with the $^{40}Ar/^{39}Ar$ ages of 129.0 ± 0.8 Ma for sample JCG-1 and 130.7 ± 0.4 Ma for sample JCG-5 within errors (14), which lie ∼2 m and ∼6 m, respectively, below that *Protopteryx*-bearing layer (Fig. 3*C*).

Timing of the Oldest Enantiornithine and Ornithuromorph Birds. During the past two decades, discoveries of the extraordinarily well-preserved bird fossils of the Jehol Biota have provided important insights into our understanding of the biology and morphology of the oldest known avifauna (3, 16, 17, 29). Our SIMS U-Pb zircon dates, coupled with previously obtained $^{40}Ar/^{39}Ar$ dates (14), have placed stringent age controls on the oldest known enantiornithine and ornithuromorph birds, which were the two dominant avian groups during the Mesozoic (17).

P. fengningensis has been recovered as the earliest branching enantiornithine in most recent cladistic analyses (16, 17, 30), exhibiting many skeletal features characteristic of more basal birds such as *Archaeopteryx* and *Confuciusornis* (16). Our age results in conjunction with the $^{40}Ar/^{39}Ar$ dates of He et al. (14) confirm that enantiornithine birds first appeared in the Jehol Biota at ∼131 Ma.

A. meemannae, the oldest record of the Ornithuromorpha, is referable to the Hongshanornithidae but phylogenetically more derived than other hongshanornithids from younger deposits (17). Our SIMS U-Pb zircon dates in combination with the $^{40}Ar/^{39}Ar$ dates of He et al. (14) show that the ornithuromorph birds first appeared in the Jehol Biota at ∼131 Ma, pushing back the first appearance datum of the Ornithuromorpha by 5 to 6 My (17).

Implications for the Differentiation and Radiation Patterns of Early Birds. As detailed above, our SIMS U-Pb zircon dates and previously obtained $^{40}Ar/^{39}Ar$ dates (14) represent the earliest absolute age for the known record of enantiornithine (16) and ornithuromorph (17) birds in the world. The enantiornithines from Las Hoyas in Spain are probably coeval, but age in this lagerstätte is determined entirely by biostratigraphic constraints without the use of precise dating methods (31). The *Protopteryx* horizon of the Huajiying Formation has also yielded two other important avian taxa. One is the basal confuciusornithine *E. zhengi* (19), which is the earliest pygostylian and beaked bird; and the other, enantiornithine *E. martini* (18), together with enantiornithine *P. fengningensis* (16), represent the first appearance datum of the Enantiornithes. All of these avian taxa are dated at ∼131 Ma, the Late Hauterivian Stage according to the Geologic Time Scale of Ogg et al. (32). These radiometric ages together with the presence of a diversity of early bird fossil lineages with drastically different morphologies indicate that by the time of the deposition of the Huajiying Formation the bird assemblage of the Early Jehol Biota had already undergone a significant phase of diversification with prominent differentiation and radiation, indicating that the origin of the Enantiornithes and Ornithuromorpha is older than previously recognized (17, 20).

Appearance and Duration of the Jehol Biota. The Jehol Biota experienced early, middle, and late stages of evolution, which were correlated to the fossil assemblages from the Dabeigou, Yixian, and Jiufotang formations, respectively (33, 34). According to the recent definition of the Jehol Biota as proposed by Pan et al. (7), the early stage should be correlated to the fossil assemblages from the Huajiying Formation (5).

In this study, sample J08-10 from the Jiecaigou section, which consists of tuffaceous sandstones and is located in the lowest part of the Huajiying Formation (Fig. 3*C*), yields an SIMS U-Pb zircon age of 135.4 ± 1.2 Ma (Fig. 5*L*). The sample lies ∼3 m above the lacustrine shale layer containing *Peipiaosteus* (Fig. 3*C*) (15). Although an earlier magmatic activity before the eruption of the tuff for the sample may lead to the inclusion of older zircon grains, as evidenced by the older age of 142.6 ± 1.5 Ma (Fig. 5*L*), the younger age of 135.4 ± 1.2 Ma most possibly signals to date the earliest occurrence of the Jehol Biota. As a result, the appearance of the Jehol Biota can at most be pushed back to ∼135 Ma.

The age of ∼135 Ma obtained in this study for the lowest Huajiying Formation of the Sichakou Basin was strengthened by numerous radiometric ages from the pre-Jehol Zhangjiakou Formation. For example, in the Luanping Basin roughly 120 km southeast of our studied Sichakou Basin, Liu et al. (22) obtained an SHRIMP U-Pb zircon age of 135.4 ± 1.6 Ma from a rhyolitic ignimbrite on the top of the Zhangjiakou Formation, and SHRIMP U-Pb zircon ages of 133.9 ± 2.5 Ma and 130.1 ± 2.5 Ma from two tuffaceous siltstone beds within the overlying Dabeigou Formation. Niu et al. (35) also obtained an SHRIMP U-Pb zircon age of 136 Ma from a rhyolitic ignimbrite on the bottom of the Zhangjiakou Formation in the Chengde and Luanping basins. Subsequently, Zhang et al. (36) obtained LA-ICP-MS U-Pb zircon ages of 135.7 ± 1.8 Ma and 135.2 ± 2.3 Ma from the strata in the Luanping Basin and proposed that the Zhangjiakou Formation could have deposited at around 135 Ma. Those radiometric ages have provided indirect but useful constraints on the age of the Early Jehol Biota.

The Yixian Formation, corresponding to the middle stage of the Jehol Biota, has yielded numerous reliable radiometric ages (8, 9, 11–13). Specifically, Chang et al. (13) obtained a $^{40}Ar/^{39}Ar$ age of 129.7 ± 0.5 Ma for a basaltic lava from the bottom of the formation.

In addition, as the late stage of the Jehol Biota the Jiufotang Formation has yielded sparse yet reliable radiometric ages. He et al. (10) reported a $^{40}Ar/^{39}Ar$ age of 120.3 ± 0.7 Ma for a tuff layer in the lower part of the formation, which is ∼1.5 m above the shale layer rich in birds and feathered dinosaurs. Subsequently, Chang et al. (13) obtained a $^{40}Ar/^{39}Ar$ age of 122.1 ± 0.3 Ma for a tuff layer from the lowermost part of the formation. Thus, the late phase of the Jehol Biota present in the Jiufotang Formation in western Liaoning can be confidently dated at ∼120 Ma (10).

Considering the above-mentioned radiometric age data together, the Jehol Biota has been placed between ∼135 and ∼120 Ma, that is, during Late Valanginian to Middle Aptian time according to the Geologic Time Scale of Ogg et al. (32). Thus, the Jehol Biota lasted for at least 15 My during the Early Cretaceous.

Methods

SIMS U-Pb Zircon Geochronology. Zircon grains were separated by conventional magnetic and density techniques to concentrate nonmagnetic, heavy fractions. The zircon of eight samples together with zircon U-Pb standard TEMORA were mounted in epoxy and polished to section the crystals in half for analysis. All zircons were documented with transmitted and reflected light micrographs as well as CL images to reveal their internal structures (Fig. 4). The mount was vacuum-coated with high-purity gold for SIMS analysis.

Measurements of U, Th, and Pb were conducted using the Cameca IMS-1280 ion microprobe at the Institute of Geology and Geophysics, Chinese Academy of Sciences, Beijing. U-Th-Pb ratios and absolute abundance data were determined relative to the standard zircon TEMORA ($^{206}Pb/^{238}U$ = 0.0669 corresponding to 417.6 Ma) (37) with a power-law relationship between Pb/U and UO_2/U (38, 39). The mass resolution used to measure Pb/Pb and Pb/U isotopic ratios was 5,400 during the analyses. A long-term uncertainty of 1.5% (1 relative standard deviation [RSD]) for $^{206}Pb/^{238}U$ measurements of the standard zircons was propagated to the unknowns (38, 40), despite that the measured $^{206}Pb/^{238}U$ error in a specific session is generally around 1% (1 RSD) or less. Measured compositions were corrected for common Pb using nonradiogenic ^{204}Pb. Corrections are sufficiently small enough to be unaffected by the choice of common Pb composition; an average of present-day crustal composition (41) was used for the common Pb assuming that the common Pb is largely due to surface contamination introduced during

sample preparation. SIMS U-Pb zircon data are presented in *SI Appendix*, Table S1. The uncertainties of the individual analysis provided in *SI Appendix*, Table S1 are reported at a 1 σ level; mean ages for pooled U/Pb and Pb/Pb analyses are quoted with 95% confidence intervals, unless otherwise noted. Data reduction was carried out using the Isoplot/Ex v. 2.49 programs (42). Details of the analysis and data-processing procedures were outlined in Li et al. (38).

Data Availability. The SIMS U-Pb age data in this paper are available in EarthRef Digital Archive, https://earthref.org/ERDA/2421/, and are also provided in *SI Appendix*, Table S1.

ACKNOWLEDGMENTS. This work was supported by the National Natural Science Foundation of China (Grants 41688103 and 41425013), and the Strategic Priority Program (B) of the Chinese Academy of Sciences (Grant XDB18030505). This paper is a contribution to the International Geoscience Programme 679.

1. Z. Zhou, P. M. Barrett, J. Hilton, An exceptionally preserved Lower Cretaceous ecosystem. *Nature* **421**, 807–814 (2003).
2. M. A. Norell, X. Xu, Feathered dinosaurs. *Annu. Rev. Earth Planet. Sci.* **33**, 277–299 (2005).
3. Z. H. Zhou, F. C. Zhang, Mesozoic birds of China—a synoptic review. *Vertebr. Palasiat.* **44**, 74–98 (2006).
4. Z. H. Zhou, Y. Wang, Vertebrate diversity of the Jehol Biota as compared with other lagerstätten. *Sci. China Earth Sci.* **53**, 1894–1907 (2010).
5. Z. H. Zhou, The Jehol biota, an early cretaceous terrestrial lagerstätte: New discoveries and implications. *Natl. Sci. Rev.* **1**, 543–559 (2014).
6. J. K. O'Connor, The trophic habits of early birds. *Palaeogeogr. Palaeoclimatol. Palaeoecol.* **513**, 178–195 (2019).
7. Y. H. Pan, J. G. Sha, Z. H. Zhou, F. T. Fürsich, The Jehol Biota: Definition and distribution of exceptionally preserved relicts of a continental Early Cretaceous ecosystem. *Cretac. Res.* **44**, 30–38 (2013).
8. C. C. Swisher III, Y. Q. Wang, X. L. Wang, X. Xu, Y. Wang, Cretaceous age for the feathered dinosaurs of Liaoning, China. *Nature* **400**, 58–61 (1999).
9. C. C. Swisher III *et al*., Further support for a cretaceous age for the feathered dinosaur beds of Liaoning, China: New $^{40}Ar/^{39}Ar$ dating of the Yixian and Tuchengzi formations. *Chin. Sci. Bull.* **47**, 136–139 (2002).
10. H. Y. He *et al*., Timing of the Jiufotang formation (Jehol group) in Liaoning, northeastern China, and its implications. *Geophys. Res. Lett.* **31**, L12605 (2004).
11. H. Y. He *et al*., $^{40}Ar/^{39}Ar$ dating of Lujiatun bed (Jehol group) in Liaoning, northeastern China. *Geophys. Res. Lett.* **33**, L04303 (2006).
12. R. X. Zhu, Y. X. Pan, R. P. Shi, Q. S. Liu, D. M. Li, Paleomagnetic and $^{40}Ar/^{39}Ar$ dating constraints on the duration of the Sihetun fossil-bearing lake sediments, northeastern China. *Cretac. Res.* **28**, 171–176 (2007).
13. S. C. Chang, H. C. Zhang, P. R. Renne, Y. Fang, High-precision $^{40}Ar/^{39}Ar$ age for the Jehol Biota. *Palaeogeogr. Palaeoclimatol. Palaeoecol.* **280**, 94–104 (2009).
14. H. Y. He *et al*., The $^{40}Ar/^{39}Ar$ dating of the early Jehol Biota from Fengning, Hebei Province, northern China. *Geochem. Geophys. Geosyst.* **7**, Q04001 (2006).
15. F. Jin *et al*., On the horizon of *Protopteryx* and the early vertebrate fossil assemblages of the Jehol Biota. *Chin. Sci. Bull.* **53**, 2820–2827 (2008).
16. F. Zhang, Z. Zhou, A primitive enantiornithine bird and the origin of feathers. *Science* **290**, 1955–1959 (2000).
17. M. Wang *et al*., The oldest record of ornithuromorpha from the early cretaceous of China. *Nat. Commun.* **6**, 6987 (2015).
18. X. L. Wang *et al*., Insights into the evolution of rachis dominated tail feathers from a new basal enantiornithine (Aves: Ornithothoraces). *Biol. J. Linn. Soc. Lond.* **113**, 805–819 (2014).
19. F. C. Zhang, Z. H. Zhou, M. J. Benton, A primitive confuciusornithid bird from China and its implications for early avian flight. *Sci. China. Ser. D Earth Sci.* **51**, 625–639 (2008).
20. M. Wang, J. K. O'Connor, Y. Pan, Z. Zhou, A bizarre Early Cretaceous enantiornithine bird with unique crural feathers and an ornithuromorph plough-shaped pygostyle. *Nat. Commun.* **8**, 14141 (2017).
21. J. H. Yang *et al*., Constraints on the timing of uplift of the Yanshan Fold and Thrust Belt, North China. *Earth Planet. Sci. Lett.* **246**, 336–352 (2006).
22. Y. Q. Liu, P. X. Li, S. G. Tian, SHRIMP U-Pb zircon age of Late Mesozoic tuff (lava) in Luanping basin, northern Hebei, and its implications (in Chinese). *Acta Petrol. Mineral.* **22**, 237–244 (2003).
23. Y. B. Wu, Y. F. Zheng, Genesis of zircon and its constraints on interpretation of U-Pb age. *Chin. Sci. Bull.* **49**, 1554–1569 (2004).
24. A. A. Nemchin, M. S. Horstwood, M. J. Whitehouse, High-spatial-resolution geochronology. *Elements* **9**, 31–37 (2013).
25. M. J. Whitehouse, B. S. Kamber, S. Moorbath, Age significance of U-Th-Pb zircon data from early Archaean rocks of west Greenland—a reassessment based on combined ion-microprobe and imaging studies. *Chem. Geol.* **160**, 201–224 (1999).
26. J. I. Simon, P. R. Renne, R. Mundil, Implications of pre-eruptive magmatic histories of zircons for U-Pb geochronology of silicic extrusions. *Earth Planet. Sci. Lett.* **266**, 182–194 (2008).
27. T. R. Ireland, I. S. Williams, Considerations in zircon geochronology by SIMS. *Rev. Mineral. Geochem.* **53**, 215–241 (2003).
28. X. H. Li, X. M. Liu, Y. S. Liu, L. Su, W. D. Sun, Accuracy of LA-ICPMS zircon U-Pb age determination: An inter-laboratory comparison. *Sci. China Earth Sci.* **58**, 1722–1730 (2015).
29. Y. Pan *et al*., Molecular evidence of keratin and melanosomes in feathers of the Early Cretaceous bird *Eoconfuciusornis*. *Proc. Natl. Acad. Sci. U.S.A.* **113**, E7900–E7907 (2016).
30. Z. Zhou, J. Clarke, F. Zhang, Insight into diversity, body size and morphological evolution from the largest Early Cretaceous enantiornithine bird. *J. Anat.* **212**, 565–577 (2008).
31. F. Knoll *et al*., A diminutive perinate European Enantiornithes reveals an asynchronous ossification pattern in early birds. *Nat. Commun.* **9**, 937 (2018).
32. J. G. Ogg, G. M. Ogg, F. M. Gradstein, *A Concise Geologic Time Scale 2016*, (Elsevier, Amsterdam, 2016).
33. P. J. Chen, Distribution and migration of the Jehol fauna with reference to non-marine Jurassic-Cretaceous boundary in China (in Chinese, abstract in English). *Acta Palaeontologica Sin.* **27**, 659–683 (1988).
34. Z. H. Zhou, Evolutionary radiation of the Jehol Biota: Chronological and ecological perspectives. *Geol. J.* **41**, 377–393 (2006).
35. B. G. Niu, Z. J. He, B. Song, J. S. Ren, SHRIMP dating of the Zhangjiakou Formation volcanic rocks and implications (in Chinese). *Geol. Bull. China* **22**, 140–141 (2003).
36. H. Zhang, H. L. Yuan, Z. C. Hu, X. M. Liu, C. R. Diwu, U-Pb zircon dating of the Mesozoic volcanic strata in Luanping of North Hebei and its significance (in Chinese). *Earth Sci. J. China Univ. Geosci.* **30**, 707–720 (2005).
37. L. P. Black *et al*., TEMORA 1: A new zircon standard for Phanerozoic U-Pb geochronology. *Chem. Geol.* **200**, 155–170 (2003).
38. X. H. Li *et al*., Precise determination of Phanerozoic zircon Pb/Pb age by multicollector SIMS without external standardization. *Geochem. Geophys. Geosyst.* **10**, Q04010 (2009).
39. H. Jeon, M. J. Whitehouse, A critical Evaluation of U-Pb calibration Schemes used in SIMS zircon geochronology. *Geostand. Geoanal. Res.* **39**, 443–452 (2015).
40. Y. N. Yang, Q. L. Li, Y. Liu, G. Q. Tang, X. X. Ling, Zircon U-Pb dating by secondary ion mass spectrometry (in Chinese with English abstract). *Earth Sci. Front* **21**, 81–92 (2014).
41. J. S. Stacey, J. D. Kramers, Approximation of terrestrial lead isotope evolution by a two-stage model. *Earth Planet. Sci. Lett.* **26**, 207–221 (1975).
42. K. R. Ludwig, *Users Manual for Isoplot/Ex Rev. 2.49, Spec. Publ. 1a*, (Berkeley Geochronology Center, Berkeley, CA, 2001).